14th Australasian Fluid Mechanics Conference
Adelaide University, Adelaide, Australia
10-14 December 2001

Computing Flow in a Spiral Particle Separator

Y. M. Stokes[1]

[1]Department of Applied Mathematics
Adelaide University, South Australia, 5005 AUSTRALIA

Abstract

To achieve improvements in the design of spiral particle separators, used in the mineral processing industry, it is necessary to have a good understanding of the fluid flow in them and the factors that affect it. To this end, we are developing computational techniques for determining the flow in a spiral channel of general geometry, including the complex free-surface shape. These can then be used to investigate how the flow, and ultimately separation, is affected by geometrical parameters and fluid flow properties.

Introduction

Spiral particle separators are used in the mineral processing industry to separate particles (e.g. of coal) of different sizes and densities. A separator consists of a channel wound about a vertical axis as shown in figure 1. A slurry of water and particles enters at the top and flows under gravity down the channel.

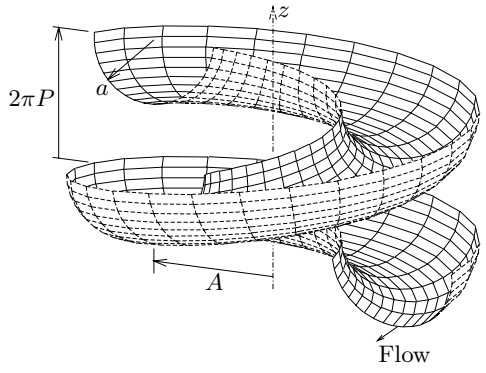

Figure 1: A helical channel a of semi-circular cross-section.

In addition to the primary axial flow down the channel, a secondary flow across the channel also develops, shown in figure 2. As explained in [3], the interaction between the fluid flow and the particles results in separation of large/heavy and small/light particles. Light particles are carried in the cross flow from the inner region of the channel (nearest the vertical axis) to the outer region; once here they take considerable time to settle to the bottom of the channel where they can be picked up in the cross flow and carried back into the inner region, during which time they are carried by the primary flow down and out of the separator. Conversely, heavy particles in the outer channel region will quickly fall to the bottom of the channel and be carried by the cross flow to the inner region; here they are too heavy to be picked up and carried back into the outer region and hence they remain in the inner region and are carried by the primary flow down the separator. Thus the particles are separated into

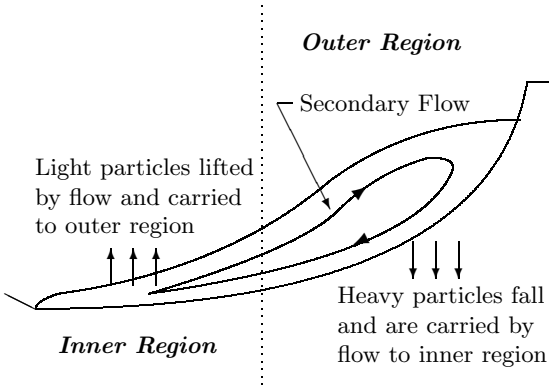

Figure 2: Secondary flow and separation mechanism (after Holland-Batt [3]).

two groups — large/heavy and small/light.

The design of these particle separators is critical to their effective operation and has been the subject of both experimental and computational studies over the last two decades [3, 4, 5, 6, 9, 10, 11]. In particular, in recent years computational fluid dynamics in three dimensions has been used to simulate such flows [6, 9], most recently with turbulence modelling included [10]. However, there is a need for a more basic analysis, including parameter studies, to determine the critical geometrical factors that influence separator operation. Some of our work to develop techniques for this type of analysis was reported in [11], and is continued here with a new technique for determining the points at which the free surface contacts the channel wall.

It is clear from the discussion above that the fluid flow is critical to the operation of a spiral separator and hence we first try to compute and understand it — in the absence of particles. Our methodology follows that used in studies of flow in closed coiled pipes [1, 2, 7] in first finding a steady-state solution that is also independent of axial position. This permits a two-dimensional analysis in the cross-section plane. A significant part of the solution process is determining the free-surface profile of the fluid in the channel, making this analysis substantially different from and more complex than fully developed flows in closed pipes. The shape of the free surface is primarily determined by the curvature of the helix and the flow rate, so that, at this stage, we ignore surface tension.

A Mathematical Model

As in [11] we consider a channel of half-width a, helically wound about the vertical z-axis with helix radius A and pitch $2\pi P$ (see figure 1), and with gravity acting in the $-z$ direction. Defining the dimensionless parameter $\lambda = P/A$ and the Reynolds number $\mathcal{R} = Ua/\nu$, where U is a characteristic axial flow velocity and ν is the kine-

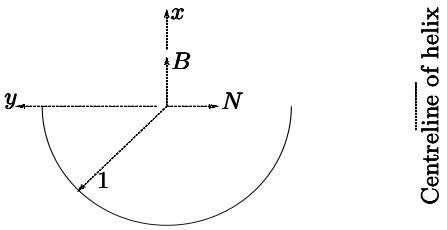

Figure 3: Cross section of a semi-circular channel showing the coordinate system; N and B are the normal and binormal vectors of the helical channel centreline with tangent directed out of the page.

matic viscosity of the fluid, we assume small dimensionless curvature ϵ and small torsion such that $\lambda/R = \mathrm{O}(\epsilon)$. Although the methodology discussed below is applicable for a channel of any cross-section shape we assume a semi-circular channel.

The dimensionless equations for this problem are given in [11] and are repeated here for convenience. The coordinate system in a cross-section of the channel is shown in figure 3, and lengths are normalised to give a channel radius of 1. Then we have the continuity equation

$$\frac{\partial v}{\partial x} + \frac{\partial w}{\partial y} = 0 \tag{1}$$

and the Navier-Stokes equations

$$v\frac{\partial u}{\partial x} + w\frac{\partial u}{\partial y} = \nabla^2 u - \frac{\lambda\mathcal{R}}{\mathcal{F}^2\sqrt{1+\lambda^2}}, \tag{2}$$

$$v\frac{\partial v}{\partial x} + w\frac{\partial v}{\partial y} = -\frac{\partial p}{\partial x} + \nabla^2 v - \frac{\mathcal{R}^2}{\mathcal{F}^2\sqrt{1+\lambda^2}}, \tag{3}$$

$$v\frac{\partial w}{\partial x} + w\frac{\partial w}{\partial y} - \frac{1}{2}Ku^2 = -\frac{\partial p}{\partial y} + \nabla^2 w, \tag{4}$$

where u is the axial flow velocity (scaled with U), v and w are the secondary flow velocity components (scaled with $U/\mathcal{R}$) in the x and y directions respectively, p is the pressure (scaled with $\rho U^2/\mathcal{R}^2$), $\mathcal{F} = U/\sqrt{ag}$ is the Froude number and $K = 2\epsilon\mathcal{R}^2$ is the Dean number associated with the centrifugal force acting on the flow.

On the channel wall we have the no-slip boundary conditions

$$u = v = w = 0 \tag{5}$$

and on the free surface with normal vector $(0, n^x, n^y)$ we have (ignoring surface tension) the zero-stress conditions

$$n^x\frac{\partial u}{\partial x} + n^y\frac{\partial u}{\partial y} = 0, \tag{6}$$

$$-pn^x + 2n^x\frac{\partial v}{\partial x} + n^y\left(\frac{\partial w}{\partial x} + \frac{\partial v}{\partial y}\right) = 0, \tag{7}$$

$$-pn^y + n^x\left(\frac{\partial w}{\partial x} + \frac{\partial v}{\partial y}\right) + 2n^y\frac{\partial w}{\partial y} = 0, \tag{8}$$

and the kinematic condition

$$vn^x + wn^y = 0, \tag{9}$$

i.e. no component of velocity normal to the free surface.

Solution Methodology

Under assumptions of small curvature and torsion when the free surface will be close to flat, an analytic solution exists for channels of semi-circular cross section [11, 13]. Defining

$$G = \frac{\lambda\mathcal{R}}{\mathcal{F}^2\sqrt{1+\lambda^2}},$$

the secondary flow components are given by $(v, w) = (\psi_y, -\psi_x)$ with the stream function ψ given by

$$\psi = -\frac{K}{9216}G^2 x\left(1-x^2-y^2\right)^2\left(4-x^2-y^2\right), \tag{10}$$

and the free surface shape is given by

$$x = \left(\frac{K}{768}\frac{G\mathcal{R}}{\lambda}\right) y\left(15-8y^2+3y^4\right). \tag{11}$$

However, for channels of general cross-section shape numerical methods must be used.

The numerical solution methodology adopted in [11] is to first guess a free surface shape and then solve (1)–(4) over the flow domain, subject to boundary conditions (5)–(8), using the finite element package *Fastflo*. The velocity field so obtained is then used to advance the mesh to give a new free surface shape and flow domain on which this process is repeated. Iteration stops when the integral of the square of the normal velocity component over the free surface, which we call the 'flux-squared', falls below some suitably chosen tolerance. At this stage, the flow is (very nearly) tangential to the free surface over its entire length and boundary condition (9) is (very nearly) satisfied.

However, as discussed in [11], this methodology has an associated difficulty: when initially guessing the free surface shape, we fix the points at which the free surface contacts the channel wall for all future time, since the no-slip wall boundary condition and the method used to update the flow domain does not permit them to move. If these points are not located accurately then, no matter how many iterations of the solution process, the free surface shape will be inaccurate and there will always be some flux through the free surface — at least locally in their vicinity.

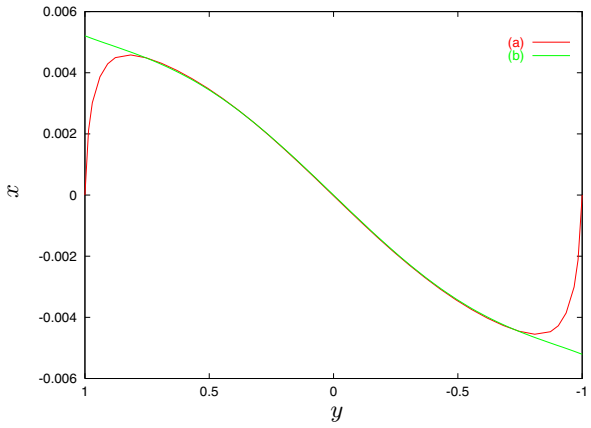

Figure 4: Free surface shape for a flow with $K = 2$, $G = 2$, $G\mathcal{R}/\lambda = 20$. (a) Numerical solution starting with a flat free surface and (b) analytic solution (11).

The effects of starting with a horizontal free surface for a semi-circular channel of small curvature and torsion (for which we have an analytic solution with which to

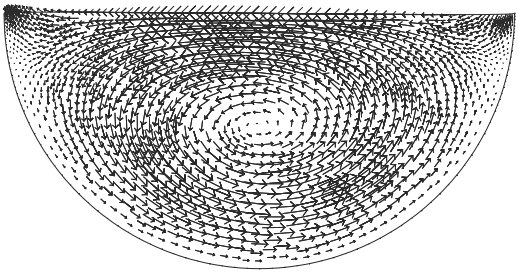

Figure 5: Velocity field corresponding to curve (a) in figure 4, showing flux through the free surface at corners due to initial inaccurate location of the points where the free surface contacts the channel wall.

compare) are shown in figures 4 and 5. The free surface shape is quite comparable with the analytic solution excepting locally near the points $(x, y) = (0, \pm 1)$ where the free surface is pinned to the channel wall. In these regions we also see a velocity component normal to the free surface, whereas the flow is tangential to the free surface away from the wall contact points. This computation was deemed to have converged when the flux-squared was just below 10^{-6}.

Zero-Pressure Corner Condition

It is clear that we need some condition by which to adjust the points of contact between the free surface and channel wall during the solution process.

Consider for a moment steady flow down a straight (zero curvature) inclined channel. There is no secondary flow in such a channel and the free surface will be horizontal [8]. On the free surface, the zero-stress boundary conditions (6)–(8) reduce to $p = 0$, as we would expect from physical considerations; in the absence of surface tension, a non-zero pressure at the free surface would drive a distortion of the free surface shape.

Of course, in a channel of non-zero curvature where a secondary flow exists, the zero-stress boundary conditions demand that pressure be non-zero where there is flow tangential to the free surface. For some free surface flows there is a mild pressure singularity at the point where a free surface meets a no-slip wall [12], but then the free surface is continuously deforming over time. Since for the free surface flow being considered here, we seek a free surface shape which does not vary in time and, in the corners where the free surface meets the channel wall, a no-slip wall requires there be no flow there, we expect the pressure to go to zero at these corners. This is readily seen from the analytic solution for a semi-circular channel of small curvature and small torsion with a nearly horizontal free surface. Since the free surface is very close to horizontal with normal $(1, 0)$, equation (7) reduces to the zero normal stress condition on $x = 0$,

$$-p + 2\frac{\partial^2 \psi}{\partial x \partial y} = 0. \tag{12}$$

Then substituting (10) gives

$$p = \frac{12K}{9216} G^2 y(1 - y^2)(3 - y^2) \tag{13}$$

on $x = 0$, and at the corners $(0, \pm 1)$ we have $p = 0$.

Thus, we use the corner pressure to move the free surface attachment points — a positive pressure indicates that the attachment point should rise and a negative pressure indicates that it should fall. To determine the vertical displacement of a contact point we compute

$$\Delta x = \left(\frac{p}{\rho g}\right) \beta, \tag{14}$$

which derives from the formula for hydrostatic pressure $p - \rho g x = 0$; β is a parameter that is used to control the amount of mesh adjustment and prevent too much mesh distortion. The contact points are also moved horizontally so that they remain on the channel wall. This condition is applied only at the free surface to wall contact points; everywhere else the mesh is still advanced in accordance with the velocity field as before.

Preliminary Results

Implementing the zero-pressure corner condition in our *Fastflo* code was quite straight forward. However, to prevent too much mesh distortion and to keep the displacement of the corner points commensurate with the displacement of nearby mesh nodes, the value of the parameter β needs to be adjusted throughout the computation. This adjustment has been done manually so far, by graphically comparing the displacement of corner nodes and neighbouring nodes on the free surface during the course of the computations, and increasing or decreasing the value as necessary. Further work is needed to automate this process.

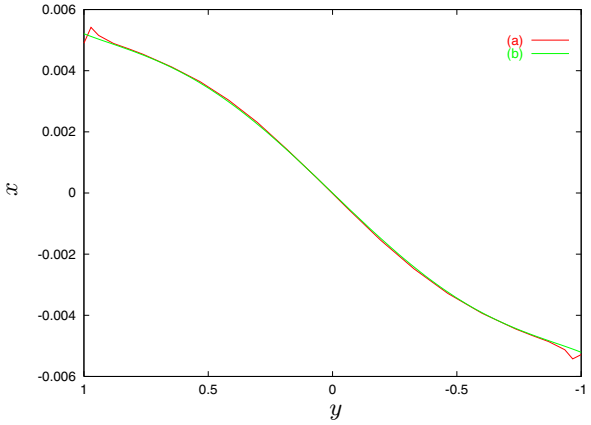

Figure 6: Free surface shape for a flow with $K = 2$, $G = 2$, $G\mathcal{R}/\lambda = 20$ after applying the $p = 0$ condition at the corners. (a) Numerical solution starting with a flat free surface and (b) analytic solution (11).

Our preliminary results, seen in figures 6 and 7, show the technique to be quite promising. With careful adjustment of β, the solution shown in these figures was obtained with considerably fewer iterations than were required before implementing the zero-pressure corner condition. The flux-squared is now about 10^{-10} — a substantial improvement on the value of 10^{-6} seen earlier. There is a kink in the free surface near the corners (see figure 6) due to the different conditions applied at the corners compared with elsewhere along the free surface but, overall, the comparison with the analytic solution, especially near the corners, is excellent.

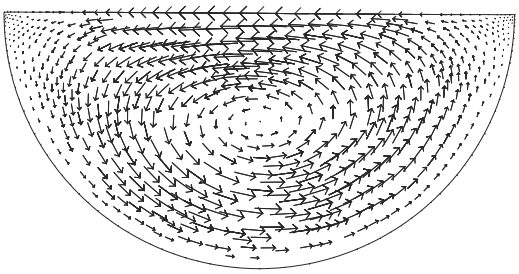

Figure 7: Velocity field corresponding to curve (a) in figure 6. With the $p = 0$ corner condition, the free surface to wall contact points have been found and the flow is (very nearly) tangential to the free surface over its full length, including near the corners.

Conclusions

From the analysis so far for semi-circular channels of small curvature and torsion, the use of a zero pressure condition at the corners, where the free surface meets the channel wall, appears to be an effective way of determining the free surface to wall contact points. Further work is in progress to prove and demonstrate the validity of the zero-pressure condition at the free surface to wall contact points for general channel geometries, and to refine and automate the method. It is also noted that the implementation of this condition, as presented here, does not guarantee conservation of mass. This is a matter that requires further investigation.

This work has focussed on steady laminar flow in a spiral channel. There is considerable evidence [3] that the flow in a spiral separator is turbulent. However, the development of these computational techniques will enable us to look at how the flow in a spiral channel changes with changes in geometrical parameters and fluid properties, and gain some insight into the specific geometrical parameters that impact upon proper separator operation. We also hope to progress to a consideration of flow stability to small disturbances and hence determine the conditions under which the flow can be expected to become turbulent.

Acknowledgements

Funding through an ARC postdoctoral fellowship is gratefully acknowledged.

References

[1] Germano, M., On the effect of torsion on a helical pipe flow. *J. Fluid Mech.*, **125**, 1982, 1–8.

[2] Germano M., The Dean equations extended to a helical pipe flow. *J. Fluid Mech.*, **203**, 1989, 289–305.

[3] Holland-Batt, A.B., Spiral separation: theory and simulation, *Trans. Instn Min. Metall. (Sect. C: Mineral Process. Extr. Metall.)*, **98**, 1989, C46–C60.

[4] Holtham, P.N. Flow visualisation of secondary currents on spiral separators, *Min. Eng.*, **3**, 1990, 279–286.

[5] Holtham, P.N., Primary and secondary fluid velocities on spiral separators, *Min. Eng.*, **5** 1992, 79–91.

[6] Jancar, T., Fletcher, C.A.J., Holtham, P.N. and Reizes, J.A., Computational and experimental investigation of spiral separator hydrodynamics, *Proc. XIX Int. Mineral Proc. Congress*, San Francisco, 1995.

[7] Kao, H.C., Torsion effect on fully developed flow in a helical pipe, *J. Fluid Mech.*, **184**, 1987, 335–356.

[8] Kuo, Y. and Tanner, R.I., Laminar Newtonian flow in open channels with surface tension, *Int. J. Mech. Sci.*, **14**, 1972, 861–873.

[9] Matthews, B.W., Fletcher, C.A.J., Partridge, A.C. and Jancar, T., Computational simulation of spiral concentrator flows in the mineral processing industry, *Chemeca '96*, 1996.

[10] Matthews, B.W., Fletcher, C.A.J. and Partridge, A.C., Computational simulation of fluid and dilute particulate flows on spiral concentrators, *Inter. Conf. on CFD in Mineral & Metal Processing and Power Generation*, CSIRO, 1997, 101–109.

[11] Stokes, Y.M., Flow in spiral channels of small curvature and torsion, *IUTAM Conf. on Free Surface Flows*, Birmingham, July 2000.

[12] Stokes, Y.M., Very viscous flows driven by gravity with particular application to slumping of molten glass, *PhD Thesis*, University of Adelaide, 1998, 39–40.

[13] Tuck, E.O., Personal communication, 1998.